Analyzing μ-Calpain induced proteolysis in a myofibril model system with vibrational and fluorescence spectroscopy

Petter Vejle Andersen [a]*, Jens Petter Wold [a], Eva Veiseth-Kent [a]

[a] Nofima AS, Osloveien 1, 1430 Ås, Norway

E-mail adresses:

Petter Vejle Andersen: petter.andersen@nofima.no

Jens Petter Wold: jens.petter.wold@nofima.no

Eva Veiseth-Kent: eva.veiseth-kent@nofima.no

*Corresponding author at: Nofima AS, Osloveien 1, 1430 Ås, Norway. Tel.: +47 64 97 04 90.

ABSTRACT

Degree of post-mortem proteolysis influences overall meat quality (e.g. tenderness and water holding capacity). Degradation of isolated pork myofibril proteins by μ-Calpain for 0, 15 or 45 min was analyzed using four spectroscopic techniques; Raman, Fourier transform infrared (FT-IR), near infrared (NIR) and fluorescence spectroscopy. Sodium dodecyl sulfate polyacrylamide gel electrophoresis was used to determine degree of proteolysis. The main changes detected by FT-IR and Raman spectroscopy were degradation of protein backbones manifested in the spectra as an increase in terminal carboxylic acid vibrations, a decrease in CN vibration, as well as an increase in skeletal vibrations. A reduction in β-sheet secondary structures was also detected, while α-helix secondary structure seemed to stay relatively unchanged. NIR and fluorescence were not suited to analyze degree of proteolysis in this model system.

Keywords

Myofibrils; proteolysis; proteins; vibrational spectroscopy; fluorescence

1. INTRODUCTION

The degree of post-mortem proteolysis in meat has been linked to important quality parameters of fresh meat, such as water holding capacity (Calvo, Toldra, Aristoy, Lopez-Bote, & Rey, 2016; Huff-Lonergan & Lonergan, 2005; Hughes, Oiseth, Purslow, & Warner, 2014; Kristensen & Purslow, 2001; Melody et al., 2004) and tenderness (Huff Lonergan, Zhang, & Lonergan, 2010; Koohmaraie, 1992; Moczkowska, Poltorak, & Wierzbicka, 2017; Taylor, Geesink, Thompson, Koohmaraie, & Goll, 1995; Veiseth-Kent, Hollung, Ofstad, Aass, & Hildrum, 2010). It is therefore of interest to analyze the degree of proteolysis in intact meat at a speed that would enable measurements on product flow normally used in meat processing, without the use of invasive and time-consuming chemical approaches, to elucidate the relationship between proteolysis and other quality parameters and to contribute towards the measurement and prediction of meat quality.

One ubiquitous proteolytic system playing a major role in muscle tissue is the calpain system, mainly consisting of the Ca^{2+} requiring cysteine proteases μ-Calpain and m-Calpain, and the calpain-specific inhibitor Calpastatin (Goll, Thompson, Li, Wei, & Cong, 2003). The calpain system has been identified and shown to be active in post-mortem porcine muscles (Ouali & Talmant, 1990), additionally, μ-Calpain has been shown to be active under post-mortem conditions (i.e. pH 5.5 and 4°C) (Koohmaraie, Schollmeyer, & Dutson, 1986). Substrates for μ-Calpain in muscle tissue are many, and some important ones related to meat quality includes nebulin, titin, vinculin, desmin (Taylor et al., 1995) and troponin-T (Olson, Parrish, Dayton, & Goll, 1977), while degradation of actin, myosin heavy chain and myosin light chain proteins have been observed in purified myofibrils incubated with μ-Calpain (Lametsch, Roepstorff, Moller, & Bendixen, 2004).

During proteolysis, proteins are degraded by cleavage of the C-N bond in the protein backbone, resulting in the formation of new terminal amino and carboxylate groups, which is a process that can potentially be followed using spectroscopic techniques. Another consequence of proteolysis is the disruption of protein structure, in particular secondary structure, of which both Raman and Fourier-transform infrared (FT-IR) spectroscopy are well suited to analyze (Barth, 2007a; Krimm & Bandekar, 1986). Recent studies have shown promise for FT-IR spectroscopy to predict protein and peptide size in laboratory scale enzymatic hydrolysis of meat by-products (Bocker, Wubshet, Lindberg, & Afseth, 2017; Wubshet et al., 2017). However, there is a limited number of studies investigating the relationship between Raman and FT-IR spectroscopy and proteolysis in meat, and most of these focus on determining degree of proteolysis in various dry-cured ham products (e.g. Moller, Parolari, Gabba, Christensen, & Skibsted,

2003; Prevolnik et al., 2011) or bulk changes in spectra following ageing (e.g. Beattie, Bell, Borggaard, & Moss, 2008). Near infrared (NIR) and fluorescence spectroscopy do not contain as much information about protein structure as Raman or FT-IR spectroscopy, but both methods are sensitive to some features of proteins. For instance, NIR spectroscopy contain absorption bands from amide I and amide II protein structures (Li-Chan, Ismail, Sedman, & van de Voort, 2002), while fluorescence spectroscopy contains information about certain amino acids microenvironment (Christensen, Norgaard, Bro, & Engelsen, 2006), both of which can contribute to analysis of proteolysis in meat.

The aim of this study was to investigate potential for spectroscopic techniques to determine degree of proteolysis in proteins isolated from pork and to establish which spectroscopic regions, which are affected by degree of proteolysis. To achieve this, we used four different spectroscopic techniques; FT-IR, Raman, NIR and fluorescence, to analyze changes in a myofibril model system, containing isolated myofibril proteins from pig muscle, incubated with μ-Calpain and Ca^{2+}. Using a model system allows for a targeted analysis of the muscle components that are predominantly altered during conversion from muscle to meat, specifically the myofibrillar proteins. In addition, the model system has the benefit of being relatively homogenous and experimental parameters can more easily be controlled. On the other hand, there are some drawbacks concerning e.g. the loss of muscle structure and other muscle components that will affect the spectroscopic results in real meat tissue.

2. MATERIALS AND METHODS

2.1 Animals, myofibril isolation and sample preparation

Myofibril isolates were prepared from five pigs as described by Andersen, Veiseth-Kent, and Wold (2017). In short, *Longissimus thoracis et lumborum* was excised and approx. 20 g was homogenized, washed in three different buffers (Pyrophosphate relaxing buffer: 2mM $Na_4P_2O_7$, 2 mM $MgCl_2$, 2 mM triethylene glycol diamine tetraacetic acid, 10 mM Tris(hydroxymethyl)aminomethane maleate salt, 0.5 mM dithiothreitol, 0.1 mM phenylmethanesulfonyl fluoride, pH 6.8; Extraction buffer: 2 mM $MgCl_2$, 2 mM triethylene glycol diamine tetraacetic acid, 10 mM Tris(hydroxymethyl)aminomethane maleate salt, 0.5 mM dithiothreitol, pH 6.8; and Triton X-100 buffer: Extraction buffer supplemented with 0.02% w/v Triton X-100) and passed through a sieve to remove fat and connective tissue, before glycerol was added and samples were stored in a freezer at -20°C until further use. Samples were thawed and washed before they were used in the experiment.

Each sample was diluted to a protein concentration of ~30 mg/ml in elution buffer, and an aliquot of 3 ml was transferred to 5 ml sample tubes in nine parallels; three were used for controls, three for

intermediate proteolysis and three for extended proteolysis. Calcium chloride (300 µl, 100 mM), EDTA (200 µl, 300 mM, pH 7.6) and Calpain-1 (8 µl) (Calbiochem, cat. no. 208712) were added to the control samples, and they were subsequently vortex mixed and stored at 4°C. Calcium chloride (300 µl, 100 mM) and Calpain-1 (8 µl) were added to the intermediate and extended samples, before they were vortex mixed and incubated, while rotating, at 25°C. After 15 min incubation, 200 µl 300 mM EDTA was added to the intermediate samples before they were vortex mixed and stored at 4°C. The same procedure was applied to the remaining samples after 45 min. The experiment was conducted over three days, where samples from one pig was analyzed day one and samples from two pigs each of the two following days.

2.2 Sodium Dodecyl Sulfate Polyacrylamide Gel Electrophoresis (SDS-PAGE) and Liquid chromatography tandem-mass spectrometry (LC-MSMS)

From each sample, 200 µl was transferred to an Eppendorf tube and 200 µl treatment buffer (0.125 M Tris(hydroxymethyl)aminomethane, 4% sodium dodecyl sulfate, 20% glycerol) was added, before the sample was vortex mixed and incubated at 95°C for 5 min, mixed by pipetting and incubated at 95°C a final time for 5 min. Samples were subsequently centrifuged at 16060 g at 4°C for 20 min, the supernatant was transferred to a fresh Eppendorf tube and stored at –20°C. Protein concentration was measured using Bio-Rad Protein Assay (Bio-Rad, California, USA) microplate procedure, and protein concentration in each sample was adjusted to 1 mg/ml by mixing thawed sample and treatment buffer with DTT (0.2 M) and bromophenol blue (0.04%). Protein (20 µg) was loaded in each well when running SDS-PAGE gel electrophoresis (NuPage 12% Bis-Tris 12 well, Invitrogen).

The gels were transferred to a small container, 50 ml Coomassie blue (0.1% Coomassie Brilliant Blue G-250 dissolved in 50% methanol and 7% acetic acid) was added and they were incubated with shaking for one hour. After this incubation, the gels were washed with dH_2O and finally 100 ml of destaining buffer (20% methanol and 7% acetic acid) was added. The gels were subsequently incubated for 2 hours with shaking, and stored in dH_2O afterwards. The gels were scanned, lanes were aligned using Progenesis SameSpots version 4.5 (Nonlinear Dynamics, Newcastle upon Tyne, UK), and profiles were extracted using ImageQuant TL 1D version 7.0 (GE Healthcare, Chicago, Ill, USA).

The five most prominent protein bands that showed systematic changes between the 0 and 45 min incubations were excised from a SDS-PAGE gel. Proteins in the gel pieces were reduced (10 mM DTT) and alkylated (55 mM IAA), prior to digestion with Trypsin/Lys-C at 37 °C overnight, and finally peptide extraction was accomplished by sonication. The peptide extracts were purified and concentrated using a StageTip, C18 material filled in 200 µl pipette tips, according to Rappsilber, Mann, and Ishihama (2007)

and Yu, Smith, and Pieper (2014). Peptides were eluted with 50 µl 70 % acetonitrile (ACN) and dried completely with a speed-vac (Thermo Fisher Scientific, USA). The dried peptides were dissolved in loading solution (0.05 % TFA, 2% ACN in water) loaded on to a trap column (Acclaim PepMap 100, C18, 5µm, 100Å, 300µm i.d. x 5 mm) and then backflushed onto a 50 cm x 75 µm analytical column (Acclaim PepMap RSLC C18, 2 µm, 100 Å, 75 µm i.d. x 50 cm, nanoViper). The gradient profile used for peptide separation was from 4 to 45 % solution B (80 % CAN, 0.1 % formic acid) in 56 min at a flow rate of 300 nL/ min. The Q-Exactive mass spectrometer was set up as follows: a full scan (300-1600 m/z) at R = 70000 was followed by (up to) 10 MS2 scans at R=35000 using an NCE setting of 28. Singly charged precursors were excluded for MS/MS as were precursors with z > 5. Dynamic exclusion was set at 20 sec. Thermo raw files were converted to .mgf format using the msconvert module of ProteoWizard (http://proteowizard.sourceforge.net/), and used to search a SwissProt database (*Taxonomy other Mammalia*) on an in-house Mascot server (version 2.4). Search parameters were: i) 10 ppm/20 mamu tolerance for MS and MS/MS, respectively; ii) trypsin, allowing up to 2 missed cleavages, iii) fixed modification cysteine carbamidomethylation and variable modification methionine oxidation. The Mascot result (.dat) files were used as input for the Scaffold software (http://www.proteomesoftware.com/products/scaffold/), for convenient result visualization and validation.

2.3 Spectroscopic analysis

Spectroscopic analysis was carried out as described by Andersen et al. (2017) with the following changes:

Raman spectroscopy: 200 µl aliquots was placed on an aluminum plate and left to dry overnight in a desiccator. Confocal hole was set to 500 µm. Exposure time was set to 6 times 10 s in the range from 500 to 1800 cm^{-1}.

FT-IR spectroscopy: Two µl of sample transferred to the plate.

NIR spectroscopy: No change for measuring liquid samples. Dried samples were measured using the same instrument settings, but a spot size of 10 mm. The samples were the same as for the Raman measurements. The aluminum plate was placed in the spectrophotometer upside down, with the dried droplet sample placed in center over the sampling window of the module. Three spectra from each sample were recorded for both analyses, and the spectra were averaged for each sample prior to analyses.

Fluorescence spectroscopy: Excitation only at 292 nm in the emission range 300 – 500 nm (2 nm step size).

2.4 Pre-processing and data analysis

2.4.1 Pre-processing of spectral data and gel profiles

Pre-processing of spectral data and gel lane profiles was done to give comparable spectra for further analysis, by reducing or removing the impact of noise, scatter effects and other undesirable alterations in the spectra.

Gel lane profiles were normalized using standard normal variate (SNV) (Barnes, Dhanoa, & Lister, 1989), before correlation optimized warping with a segment size of 90 and a slack of 10 was applied to align peaks.

The FT-IR spectra were subjected to Extended Multiplicative Signal Correction (Martens & Stark, 1991) (EMSC) with replicate correction (Kohler et al., 2009) to reduce the effects of changes in light intensity and scattering, and day to day variation in the measurements. EMSC is a model based pre-processing approach which handles additive polynomial baselines (6^{th} order was used) as well as multiplicative effects in a single model. Replicate correction finds common variation across sets of replicates using singular value decomposition of EMSC corrected spectra, i.e. batches of measurements from individual days. The dominant common variation is reintroduced into the EMSC model as interferent spectra to perform a final combined modelling and correction. One sample was excluded from FT-IR analysis because of too high absorption.

Raman spectra were pre-processed by means of full extended multiplicative scattering correction (EMSC) including 6^{th} order polynomial (Liland, Kohler, & Afseth, 2016). Five spectra from each sample were averaged and subsequently smoothed by applying a Savitzky-Golay filter with four smoothing points on each side in the second order. Two samples were excluded from Raman analysis because of changes in confocal hole diameter, giving too dissimilar spectra to compare with the others. Reason for changes to confocal hole was saturation of the detector in one sample and too little signal for the detector for the other sample.

The NIR spectra from Gold Reflectance Cellkit were divided into three regions, 400 to 900 nm, 1100 to 1700 nm, and 1700 to 2350 nm, before EMSC was applied to each region separately. NIR spectra from dried samples were subjected to EMSC in the entire recorded region from 1100 to 2500 nm.

Fluorescence spectra were pre-processed only by SNV.

2.4.2 Data analysis

Principal component analysis (PCA) was utilized to verify that samples were grouped according to degree of proteolysis, meaning that changes in spectra is representative of the proteolysis-related variation in the spectra. Partial least squares regression (PLSR) was used for determining relationship between proteolysis and spectroscopic data, the procedure included an uncertainty test for revealing important variables in the model. Both analyses were cross-validated using leave-one-out procedure. FT-IR and Raman used only the important variables from uncertainty test to make the models in table 2, while NIR and fluorescence used all variables. Reference measurements for PLSR were SDS-PAGE PCA scores for principal component 1 for each sample, which represents a relative value for degree of proteolysis within the current experiment.

PCA and PLSR was performed in the following spectral regions: Raman: 500 to 1800 cm^{-1}, FT-IR: from 800 to 1800 cm^{-1}, NIR: each of the spectral regions from EMSC separately and fluorescence: excitation at 292 nm and emission 306 – 412 nm.

Data analysis was carried out using Open EMSC toolbox for MATLAB freely downloadable from http://nofimaspectroscopy.org in MATLAB version R2013b (The MathWorks, Natick, MA) and using The Unscrambler® X version 10.4 (CAMO Process AS, Norway).

3. RESULTS AND DISCUSSION

3.1 SDS-PAGE

Inspection of average lane profiles from SDS-PAGE and Coomassie staining revealed a time-dependent degradation of certain proteins (Fig. 1). Degradation of myosin heavy chain (MHC) was the most prominent, as evidenced by a decrease in the MHC band and an increase in the amount of fragmented MHC in all LC-MSMS analyzed bands. Significant degradation of MHC in isolated myofibrils has been documented before (Lametsch et al., 2004), but the degradation is limited in intact meat (Lametsch, Roepstorff, & Bendixen, 2002), meaning that potential responses in spectroscopy from MHC degradation are questionable when transferring these results to analysis of intact meat. According to the LC-MSMS analysis the concentration of intact actin decreased as incubation time increased, but the actin peak in the lane profile showed an opposite relation and this was probably caused by the increased concentration of MHC fragments in the actin band. Degradation of troponin-T followed the same pattern as degradation of MHC, with highest concentration of the intact protein at the onset of the experiment, gradually decreasing as incubation time increased, and the reverse pattern was identified for the degradation product. Degradation of troponin-T in post-mortem meat is thoroughly documented (Huff

Lonergan et al., 2010; Moczkowska et al., 2017), and the intensity of the 32 kDa degradation product can be used as a marker of overall proteolysis in meat (Olson et al., 1977).

A PCA was performed to investigate if the differences in gel lane profiles were consistent for all samples and incubation times, and what parts of the gel lanes were the most important for separating the different incubation times. Fig. 2 shows that there was a separation along PC-1 in accordance with the three incubation times, hence, the scores from PC-1 were used to represent overall protein degradation of each sample. Samples incubated for 15 and 45 min were more similar than samples incubated for 0 and 15 min, evidenced by the overlap of samples for 15 and 45 min and no overlap between 0 and 15 min for PC-1. This indicates that the proteolytic activity decreased after 15 min of incubation. Loadings from PCA for PC-1 (results not shown) reveals that the most important part of the gel profiles for separating degree of proteolysis is the amount of intact and degradation product from MHC, and to a lesser degree, troponin-T.

3.2 FT-IR spectroscopy

The FT-IR spectra had a strong protein signature, where the amide I and II peaks were prominent (Fig. 3). The center of the peaks for both amide I and amide II suggest that the protein secondary structure were predominantly α-helices (Bocker et al., 2007). To identify regions in the spectrum that are important for determining degree of proteolysis both the native spectrum and the difference spectrum (Fig. 3) were analyzed. There was a systematic change in the spectra from 0 to 15 min and 15 to 45 min, and the change was more pronounced from 0 to 15 min than for 15 to 45 min, which was in correspondence with results from SDS-PAGE.

In the difference spectra there were six peaks that are clearly related to protein modifications following proteolysis (Table 1). The same peaks were the most important for differentiating between proteolysis times in a PCA, resulting in a grouping along PC1 in the PCA scores plot (Fig. 4). To explore the link between spectroscopy and proteolysis a PLSR model was calculated (Table 2), which showed that FT-IR could predict degree of proteolysis in the model system very well (r_{cv}^2=0.92 and RMSECV = 0.78). The spectroscopic changes can be split into two categories: 1) there are direct changes following cleavage of peptide bonds, and 2) there are changes related to modifications in protein secondary structures.

Peptide bond cleavage was manifested in the spectra as an increase in absorption of carboxylate, at 1595 cm^{-1} and 1414 cm^{-1} (Guler, Dzafic, Vorob'ev, Vogel, & Mantele, 2011), and by reduced absorption of NH and CN in the amide II region (Barth, 2007a). Changes in secondary structure seemed to be in the form of

a reduction in β-sheets and a simultaneous increase in α-helix and/or disordered structures. Reduction in β-sheet absorbance was evident in the amide I peak, at 1685 and 1635 cm^{-1}, and the amide II peak, at 1533 cm^{-1}. The changes to α-helix absorption were contradictory, as there is an increase in absorption at 1650 cm^{-1} for amide I and a decrease at 1544 cm^{-1} for amide II. An explanation for the increased absorbance at 1650 cm^{-1} can be an increase in disordered secondary structures accompanied by an increase in solute exposed α-helices (Barth, 2007a), caused by calpain recognition and digestion of disordered protein structures (Tompa et al., 2004). Decrease of absorption in the amide II region is most likely a consequence of major decrease in CN and NH absorption, influencing all other features in the amide II peak. The reason for a reduction in β-sheet absorbance might be that these structures are more prone to destabilization, compared to α-helices, when the overall integrity of the protein is compromised. Skeletal stretch in proteins are generally found in the region from 1200-880 cm^{-1}(Barth, 2007b), and the absorption of the peak at 1055 cm^{-1} can be attributed to changes in secondary structure, where an increase in disordered structures at the expense of ordered structures could be causing the increase in absorption. Bocker et al. (2017) identified the skeletal stretch as a region inversely correlating to the degree of hydrolysis of different muscle hydrolysates, which is opposite of the response in the current study. This can be attributed to differences in the constituents of the analyzed samples. In the current study, a representative volume of the whole sample was used for FT-IR, while Bocker et al. (2017) used a filtered sample from the peptide-rich water phase. Meaning that Bocker et al. (2017) analyzed increasing amounts of smaller peptides, while the current study analyzed a mix of peptides and more intact proteins and protein structures, possibly causing the inverse relation between FT-IR and proteolysis in the two studies. Overall, this indicates that the skeletal stretch is an important region for analyzing degree of proteolysis.

3.3 Raman spectroscopy

Analyzing differences in Raman spectra revealed many of the same responses following proteolysis as FT-IR analysis, including the relative difference in intensity between incubation times (Fig. 5 and Table 3). PCA revealed the same areas of importance as for the difference spectra, but they were not as distinct as for FT-IR. The PLSR model from Raman was less good than for FT-IR, but shows that there was a reasonable link between Raman and degree of proteolysis in the model system. In short, there seemed to be a decrease in β-sheet vibrations, with a simultaneous increase in carboxylic acid and skeletal/α-helix vibrations. Decrease in β-sheets following proteolysis was evident in both the amide I and III peak, with a respective decrease in intensity at 1673 and 1246 cm^{-1} (Krimm & Bandekar, 1986). Intensity for COO^- at 1405 cm^{-1} and for COOH at 1720 cm^{-1} increased, reinforcing the notion that the amount of C-

terminal carboxylic acid increased (Tu, 1986). Increase in intensity at 915 cm^{-1} in the skeletal stretch region indicated an increase in α-helix structures (Tu, 1986), and can be explained by a relative increase in α-helices compared to other secondary structures as the amount of β-sheets are reduced. In addition, the intensity of amino acid side chain ring vibrations of phenylalanine (Phe) at 1003 cm^{-1} decreased following protein degradation, implying a decrease in protein concentration, but this peak does not contain any conformational information (Barrett, Peticolas, & Robson, 1978).

3.4 NIR spectroscopy

NIR spectroscopy of dried samples showed some promise in determining degree of proteolysis when examining the spectra (Fig. 6), PCA and PLSR (Table 2). This means that there is possibly enough information in the NIR spectra to distinguish larger differences in degree of proteolysis of dried samples. PCA reveals that the peak at approx. 1940 nm explains almost all of the variation in the spectra related to degree of proteolysis, and this peak is attributed to water (Buning-Pfaue, 2003). The higher absorption for lesser degree of proteolysis could be caused by higher concentration of bound water in more intact myofibrils or it could be because of changes in the conditions surrounding the water molecules, e.g. gelling properties or the size of proteins (Buning-Pfaue, 2003). This makes it difficult to pin-point the mechanism behind the NIR response.

NIR spectroscopy of liquid samples yielded poor results for all methods of investigating the spectra. It did not reveal any distinct spectral differences, PCA grouping or any good PLSR models (Table 2) related to degree of proteolysis.

3.5 Fluorescence spectroscopy

Fluorescence spectra of liquid samples (Fig. 7) seemed to differentiate between degraded and non-degraded samples, manifested as a slight shift in the emission maximum peak to higher wavelengths for degraded samples. Spectra from degraded samples overlapped at different wavelengths throughout the main peak, reinforcing the impression that fluorescence spectroscopy is not sensitive to protein degradation beyond the major changes before 15 min in the current experiment. This trend was present in PCA (not shown), but the shift to higher wavelengths was not consistent for all samples, giving a high degree of overlap in the scores plot. Results from PLSR supports the notion that the correlation was weak, as the model is not reliable when predicting degree of proteolysis (Table 2). The fluorescence peak is attributed to tryptophan (Trp) emission, and changes in maximum emission peak position of Trp is often related to microenvironment changes (Christensen et al., 2006). Trp emission peak centers at

longer wavelengths for less structured molecules, which can explain the observed change in emission peak, because the degraded proteins are less structured than their un-degraded counterparts.

4. GENERAL DISCUSSION

From the current experiment, it is evident that FT-IR spectroscopy was capable of predicting degree proteolysis in myofibrils. However, there are some concerns regarding integrating FT-IR in a meat processing plant, first, one need to overcome the obstacle of high water absorption in FT-IR, and secondly, one needs a constant atmosphere or vacuum when measuring. This can be solved by using attenuated total reflectance where the water peak at 1640 cm^{-1} is omitted in the spectra and the crystal is thoroughly cleaned between each measurement, which may be too cumbersome to be a practical solution. However, FT-IR can potentially be used as tool to screen samples for degree of proteolysis by analyzing cryosections in the laboratory.

Raman spectroscopy did not perform as well as FT-IR in PCA or PLSR, but interpretation of spectroscopic differences were consistent with results from FT-IR, which makes us believe that Raman spectroscopy can perform on a similar level as FT-IR. The poorer performance for Raman spectroscopy in the current study may be caused by less standardized measurements (e.g. by manually focusing and acquiring Raman spectra) and fewer samples included in the analysis. Regardless, both FT-IR and Raman showed the same trend in intensity changes as the degree of proteolysis did, showing larger differences early in the degradation process than later, demonstrating that there is a possible quantitative association between spectroscopy and protein degradation. Another important consideration is how plausible it is for the spectroscopic method to be used in a meat processing plant, and in this case Raman spectroscopy has several advantages, most importantly that it is not very sensitive to water in the sample, it can be used in ambient conditions and spectra can be recorded directly on the meat surface (Li-Chan, 1996). Sensitivity of Raman spectroscopy is also a subject to consider, as the Raman signal is relatively weak, and requires analyte concentration in the range of 2-20 mg/mL to get good signal using conventional Raman instruments (Li-Chan, 1996). Since the concentration of degraded proteins is relatively small compared to the total amount of proteins, and the spectroscopic response is universal in nature (not linked to specific proteins), it is possible that the specificity of Raman spectroscopy is not good enough for measurements of degree of proteolysis.

Results from FT-IR and Raman spectroscopy indicated that the spectroscopic regions affected by proteolysis were related to general changes following protein degradation (e.g. increase in C-terminals

and decrease in CN bonds), meaning that these methods could be able to analyze protein degradation independently of the proteolytic system in effect and which proteins are degraded.

Models from NIR spectroscopy performed inferior to both Raman and FT-IR on dried samples, but still seemed to contain important information regarding degree of proteolysis. The poorer performance may be caused by a higher degree of overlapping spectral features and less specific spectral information related to the important changes during protein degradation (e.g. protein secondary structure and CN vibration) in NIR spectra. Since the observed change in NIR spectra in the current study is believed to be caused by the condition of the dried samples, and not specific protein modifications, there is little reason to believe that these findings are transferrable to intact meat.

Even though Fluorescence spectroscopy is a very sensitive method, it did not perform well enough to give models of predictive value, indicating that fluorescence spectroscopy may not be suited for measuring degree of proteolysis.

As protein degradation progresses, the amount of peptide terminal groups increases, which causes a decrease in pH. This decrease in pH has been shown to not affect FT-IR spectroscopy of whey proteins (Poulsen et al., 2016), and the buffer used in the current experiment should keep pH stable, so this effect is considered negligible in the current experiment. Nevertheless, it is plausible that the spectroscopic contribution of C-terminal carboxylic acids (at approx. 1400 cm^{-1}), formed during proteolysis, will partially disappear or merge with contributions from the naturally occurring pH-decline post-mortem (Andersen et al., 2017).

5. CONCLUSION

FT-IR and Raman spectroscopy are showing promise for measuring degree of proteolysis in myofibrils, with Raman spectroscopy as the front-runner for testing and possible implementation as a part of meat quality assessment in a meat processing plant. NIR and fluorescence spectroscopy showed little promise for measuring degree of proteolysis. It is important to point out that this study only indicates that spectroscopic techniques are viable for analyzing degree of proteolysis in model systems, and that more studies are needed to make any conclusions as to the viability for measuring proteolysis in intact meat.

Acknowledgements

We thank Bjørg Narum, Vibeke Høst and Dr. Morten Skaugen for technical assistance during sampling and in the analyses, Dr. Kristian Liland for assistance in pre-processing of spectroscopic data and Dr. Ulrike Böcker for critical comments on the manuscript and interpretation of spectroscopic results. This

work was supported by the Foundation for Research Levy on Agricultural products and the Agricultural Agreement Research Fund of Norway.

6. REFERENCES

Andersen, P. V., Veiseth-Kent, E., & Wold, J. P. (2017). Analyzing pH-induced changes in a myofibril model system with vibrational and fluorescence spectroscopy. *Meat Sci, 125*, 1-9.

Barnes, R. J., Dhanoa, M. S., & Lister, S. J. (1989). Standard Normal Variate Transformation and De-Trending of near-Infrared Diffuse Reflectance Spectra. *Applied Spectroscopy, 43*(5), 772-777.

Barrett, T. W., Peticolas, W. L., & Robson, R. M. (1978). Laser Raman light-scattering observations of conformational changes in myosin induced by inorganic salts. *Biophys J, 23*(3), 349-358.

Barth, A. (2007a). Infrared spectroscopy of proteins. *Biochim Biophys Acta, 1767*(9), 1073-1101.

Barth, A. (2007b). *Methods in Protein Structure and Stability Analysis: Vibrational spectroscopy*: Nova Biomedical Books.

Beattie, J. R., Bell, S. E. J., Borggaard, C., & Moss, B. W. (2008). Preliminary investigations on the effects of ageing and cooking on the Raman spectra of porcine longissimus dorsi. *Meat Science, 80*(4), 1205-1211.

Bocker, U., Ofstad, R., Wu, Z., Bertram, H. C., Sockalingum, G. D., Manfait, M., Egelandsdal, B., & Kohler, A. (2007). Revealing covariance structures in fourier transform infrared and Raman microspectroscopy spectra: a study on pork muscle fiber tissue subjected to different processing parameters. *Appl Spectrosc, 61*(10), 1032-1039.

Bocker, U., Wubshet, S. G., Lindberg, D., & Afseth, N. K. (2017). Fourier-transform infrared spectroscopy for characterization of protein chain reductions in enzymatic reactions. *Analyst, 142*(15), 2812-2818.

Buning-Pfaue, H. (2003). Analysis of water in food by near infrared spectroscopy. *Food Chemistry, 82*(1), 107-115.

Calvo, L., Toldra, F., Aristoy, M. C., Lopez-Bote, C. J., & Rey, A. I. (2016). Effect of dietary organic selenium on muscle proteolytic activity and water-holding capacity in pork. *Meat Science, 121*, 1-11.

Christensen, J., Norgaard, L., Bro, R., & Engelsen, S. B. (2006). Multivariate autofluorescence of intact food systems. *Chem Rev, 106*(6), 1979-1994.

Goll, D. E., Thompson, V. F., Li, H., Wei, W., & Cong, J. (2003). The calpain system. *Physiol Rev, 83*(3), 731-801.

Guler, G., Dzafic, E., Vorob'ev, M. M., Vogel, V., & Mantele, W. (2011). Real time observation of proteolysis with Fourier transform infrared (FT-IR) and UV-circular

dichroism spectroscopy: Watching a protease eat a protein. *Spectrochimica Acta Part a-Molecular and Biomolecular Spectroscopy, 79*(1), 104-111.
Herrero, A. M. (2008). Raman spectroscopy a promising technique for quality assessment of meat and fish: A review. *Food Chemistry, 107*(4), 1642-1651.
Huff-Lonergan, E., & Lonergan, S. M. (2005). Mechanisms of water-holding capacity of meat: The role of postmortem biochemical and structural changes. *Meat Sci, 71*(1), 194-204.
Huff Lonergan, E., Zhang, W., & Lonergan, S. M. (2010). Biochemistry of postmortem muscle - lessons on mechanisms of meat tenderization. *Meat Sci, 86*(1), 184-195.
Hughes, J. M., Oiseth, S. K., Purslow, P. P., & Warner, R. D. (2014). A structural approach to understanding the interactions between colour, water-holding capacity and tenderness. *Meat Science, 98*(3), 520-532.
Kohler, A., Bocker, U., Warringer, J., Blomberg, A., Omholt, S. W., Stark, E., & Martens, H. (2009). Reducing Inter-replicate Variation in Fourier Transform Infrared Spectroscopy by Extended Multiplicative Signal Correction. *Applied Spectroscopy, 63*(3), 296-305.
Koohmaraie, M. (1992). The Role of Ca-2+-Dependent Proteases (Calpains) in Postmortem Proteolysis and Meat Tenderness. *Biochimie, 74*(3), 239-245.
Koohmaraie, M., Schollmeyer, J. E., & Dutson, T. R. (1986). Effect of Low-Calcium-Requiring Calcium Activated Factor on Myofibrils under Varying Ph and Temperature Conditions. *Journal of Food Science, 51*(1), 28-&.
Krimm, S., & Bandekar, J. (1986). VIBRATIONAL SPECTROSCOPY AND CONFORMATION OF PEPTIDES, POLYPEPTIDES, AND PROTEINS. [Review]. *Advances in Protein Chemistry, 38*, 181-364.
Kristensen, L., & Purslow, P. P. (2001). The effect of ageing on the water-holding capacity of pork: role of cytoskeletal proteins. *Meat Science, 58*(1), 17-23.
Lametsch, R., Roepstorff, P., & Bendixen, E. (2002). Identification of protein degradation during post-mortem storage of pig meat. *J Agric Food Chem, 50*(20), 5508-5512.
Lametsch, R., Roepstorff, P., Moller, H. S., & Bendixen, E. (2004). Identification of myofibrillar substrates for mu-calpain. *Meat Sci, 68*(4), 515-521.
Li-Chan, E. C. Y. (1996). The applications of Raman spectroscopy in food science. *Trends in Food Science & Technology, 7*(11), 361-370.
Li-Chan, E. C. Y., Ismail, A. A., Sedman, J., & van de Voort, F. R. (2002). Vibrational Spectroscopy of Food and Food Products *Handbook of Vibrational Spectroscopy*: John Wiley & Sons, Ltd.
Liland, K. H., Kohler, A., & Afseth, N. K. (2016). Model-based pre-processing in Raman spectroscopy of biological samples. *Journal of Raman Spectroscopy, 47*(6), 643-650.

Martens, H., & Stark, E. (1991). Extended Multiplicative Signal Correction and Spectral Interference Subtraction - New Preprocessing Methods for near-Infrared Spectroscopy. *Journal of Pharmaceutical and Biomedical Analysis, 9*(8), 625-635.

Melody, J. L., Lonergan, S. M., Rowe, L. J., Huiatt, T. W., Mayes, M. S., & Huff-Lonergan, E. (2004). Early postmortem biochemical factors influence tenderness and water-holding capacity of three porcine muscles. *J Anim Sci, 82*(4), 1195-1205.

Moczkowska, M., Poltorak, A., & Wierzbicka, A. (2017). The effect of ageing on changes in myofibrillar protein in selected muscles in relation to the tenderness of meat obtained from cross-breed heifers. *International Journal of Food Science and Technology, 52*(6), 1375-1382.

Moller, J. K., Parolari, G., Gabba, L., Christensen, J., & Skibsted, L. H. (2003). Monitoring chemical changes of dry-cured Parma ham during processing by surface autofluorescence spectroscopy. *J Agric Food Chem, 51*(5), 1224-1230.

Olson, D. G., Parrish, F. C., Dayton, W. R., & Goll, D. E. (1977). Effect of Postmortem Storage and Calcium Activated Factor on Myofibrillar Proteins of Bovine Skeletal-Muscle. *Journal of Food Science, 42*(1), 117-124.

Ouali, A., & Talmant, A. (1990). Calpains and Calpastatin Distribution in Bovine, Porcine and Ovine Skeletal-Muscles. *Meat Science, 28*(4), 331-348.

Poulsen, N. A., Eskildsen, C. E., Akkerman, M., Johansen, L. B., Hansen, M. S., Hansen, P. W., Skov, T., & Larsen, L. B. (2016). Predicting hydrolysis of whey protein by mid-infrared spectroscopy. *International Dairy Journal, 61*, 44-50.

Prevolnik, M., Skrlep, M., Janes, L., Velikonja-Bolta, S., Skorjanc, D., & Candek-Potokar, M. (2011). Accuracy of near infrared spectroscopy for prediction of chemical composition, salt content and free amino acids in dry-cured ham. *Meat Sci, 88*(2), 299-304.

Rappsilber, J., Mann, M., & Ishihama, Y. (2007). Protocol for micro-purification, enrichment, pre-fractionation and storage of peptides for proteomics using StageTips. *Nature Protocols, 2*(8), 1896-1906.

Rygula, A., Majzner, K., Marzec, K. M., Kaczor, A., Pilarczyk, M., & Baranska, M. (2013). Raman spectroscopy of proteins: a review. *Journal of Raman Spectroscopy, 44*(8), 1061-1076.

Taylor, R. G., Geesink, G. H., Thompson, V. F., Koohmaraie, M., & Goll, D. E. (1995). Is Z-Disk Degradation Responsible for Postmortem Tenderization. *Journal of Animal Science, 73*(5), 1351-1367.

Tompa, P., Buzder-Lantos, P., Tantos, A., Farkas, A., Szilagyi, A., Banoczi, Z., Hudecz, F., & Friedrich, P. (2004). On the sequential determinants of calpain cleavage. *J Biol Chem, 279*(20), 20775-20785.

Tu, A. T. (1986). *Spectroscopy of Biological Systems*: Wiley.

Veiseth-Kent, E., Hollung, K., Ofstad, R., Aass, L., & Hildrum, K. I. (2010). Relationship between muscle microstructure, the calpain system, and shear force in bovine longissimus dorsi muscle. *Journal of Animal Science, 88*(10), 3445-3451.

Wubshet, S. G., Mage, I., Bocker, U., Lindberg, D., Knutsen, S. H., Rieder, A., Rodriguez, D. A., & Afseth, N. K. (2017). FTIR as a rapid tool for monitoring molecular weight distribution during enzymatic protein hydrolysis of food processing by-products. [10.1039/C7AY00865A]. *Analytical Methods, 9*(29), 4247-4254.

Yu, Y., Smith, M., & Pieper, R. (2014). A spinnable and automatable StageTip for high throughput peptide desalting and proteomics.

***Table 1**. Overview of important spectroscopic responses detected by FT-IR spectroscopy related to degree of proteolysis in the current study. Arrows denote changes in intensity as a function of degree of proteolysis.*

Wavenumber (cm^{-1})	Absorbance change	Structure
1685	↓	Amide I, β-sheet, C=O [a]
1650	↑	Amide I, α-helix/disordered, C=O [b]
1595	↑	COO^- (antisymmetric) [c]
1533	↓	Amide II, β-sheet, CN [a]
1414	↑	COO^- (symmetric) [c]
1055	↑	Skeletal stretch [d]

[a] (Bocker et al., 2007).
[b] (Barth, 2007a).
[c] (Guler et al., 2011).
[d] (Barth, 2007b)

***Table 2**. Summary of performance for cross-validated PLSR models from spectroscopy vs. PC1 scores from PCA of SDS lane profiles. Only the best performing model from each spectroscopic method is shown.*

Method	n	# factors in model	r^2	RMSECV
FT-IR	36	6	0.92	0.78
Raman	27	4	0.83	1.07
NIR (dried)	43*	10	0.74	1.42
NIR (liquid)[¤]	45	4	0.10	2.61
Fluorescence	43*	2	0.25	2.27

*Two samples were removed from NIR (dried) and fluorescence PLSR because of extreme residual values.

[¤] Spectral range from 1700 nm to 2350 nm used in the model.

***Table 3**. Overview of important spectroscopic responses detected by Raman spectroscopy related to degree of proteolysis in the current study. Arrows denote changes in intensity as a function of degree of proteolysis.*

Approx. wavenumber (cm^{-1})	Absorbance change	Structure
915	↑	Skeletal stretch, CC, α-helix [a, b, c]
1003	↓	Phe [a, b, c]
1245	↓	Amide III, CN and NH, β-sheet/random coil [a, b, c]
1405	↑	COO^- [a, c]
1673	↓	Amide I, β-sheet [a, b, c]

[a] (Herrero, 2008).
[b] (Rygula et al., 2013).
[c] (Tu, 1986).

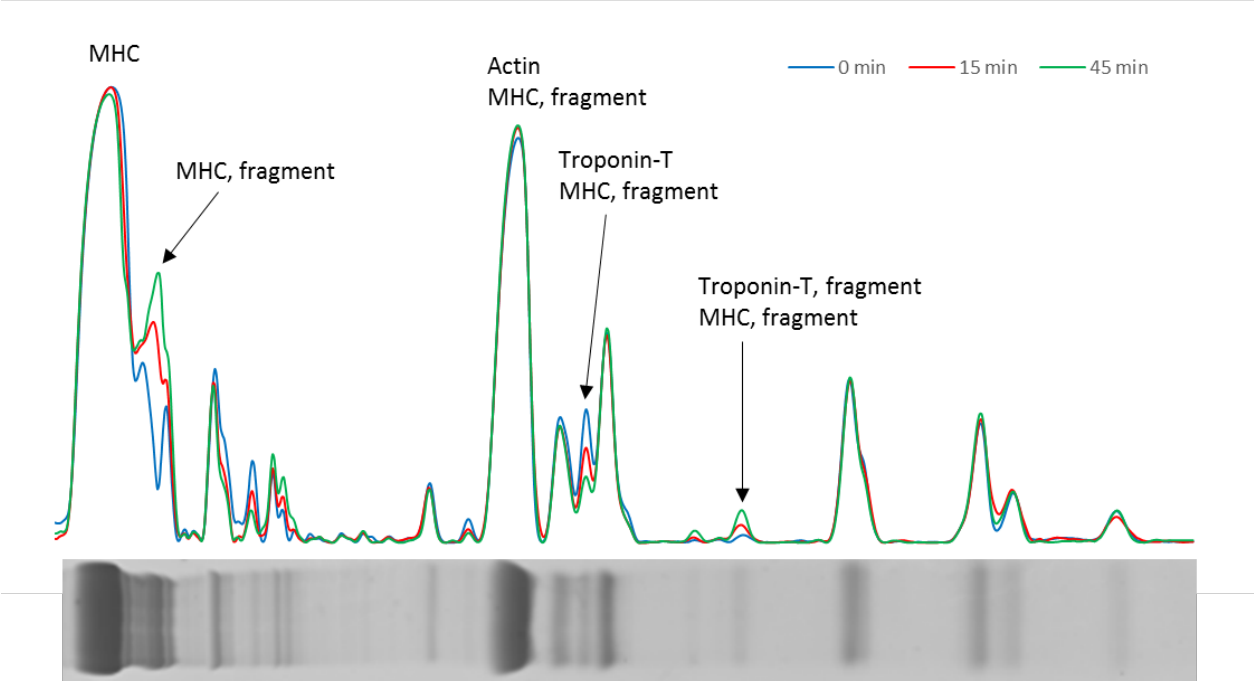

Figure 1. Average lane profiles after incubation for 0, 15 and 45 min. from SDS-PAGE analysis. The horizontal gel-lane underneath the graph is a representative sample after 45 min incubation. Full-length proteins and protein fragments with concentration changes following incubation is marked in the figure, the proteins was identified by LC-MSMS.

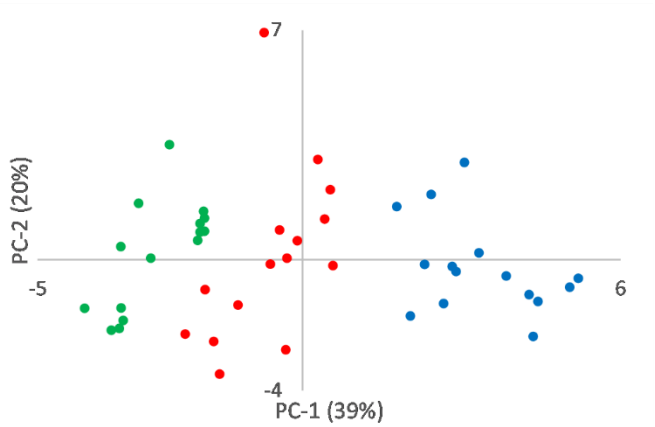

509

510 ***Figure 2.*** PCA scores plot from lane profiles. Blue dots = 0 min, red dots = 15 min and green dots = 45

511 min.

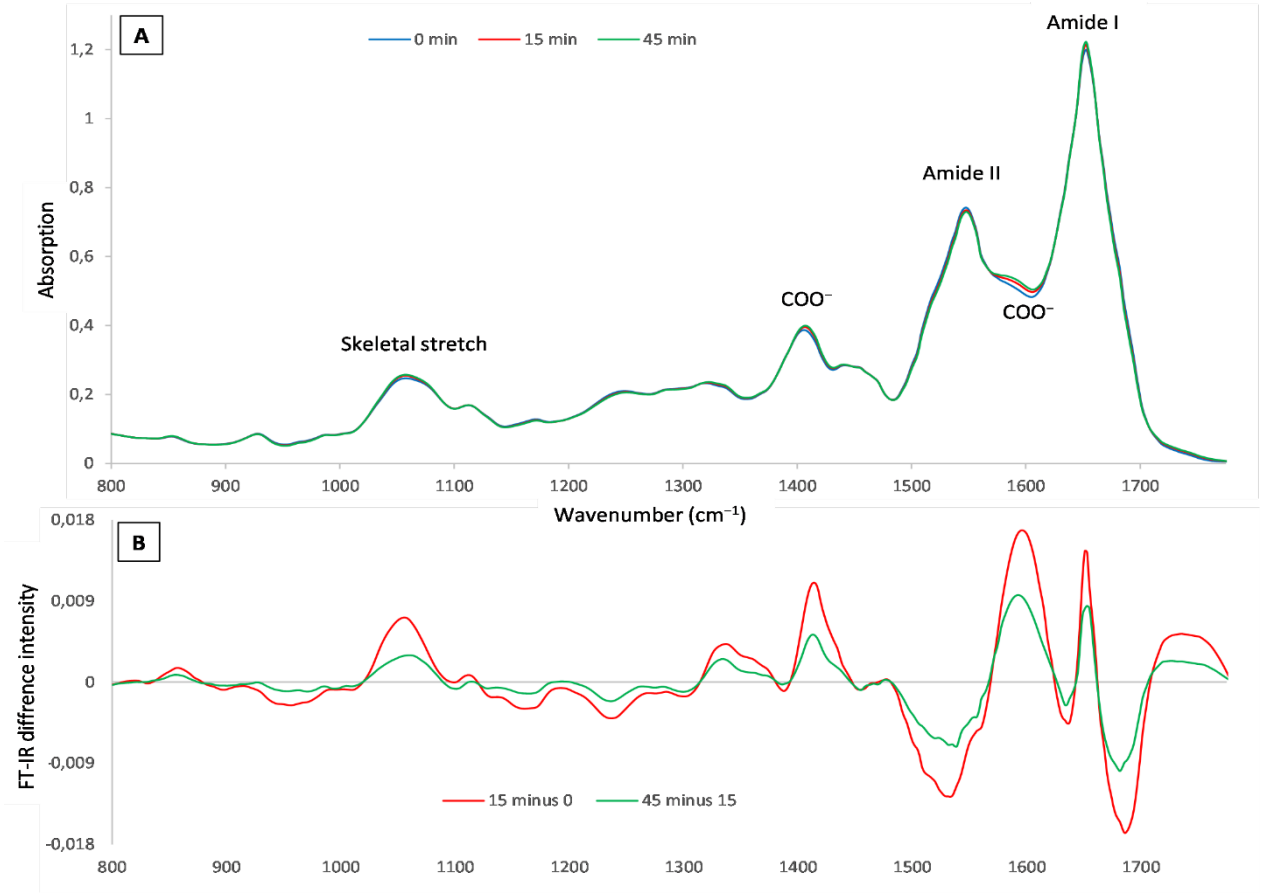

512

513 ***Figure 3. (A)*** Average spectra from FT-IR from four myofibril isolates. Peaks important for analyzing

514 degree of proteolysis are noted in the figure. ***(B)*** Difference spectra for average FT-IR spectra for each

515 incubation time, where 15 min – 0 min and 45 min – 15 min corresponds to green and red lines,

516 respectively.

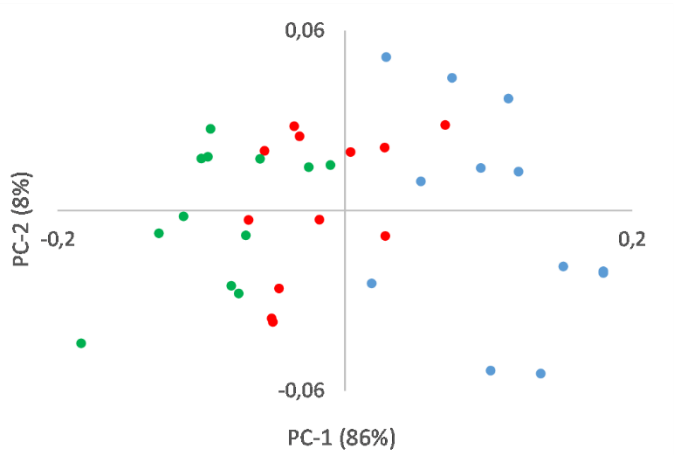

Figure 4. PCA scores plot from FT-IR spectroscopy. Blue dots = 0 min, red dots = 15 min and green dots = 45 min.

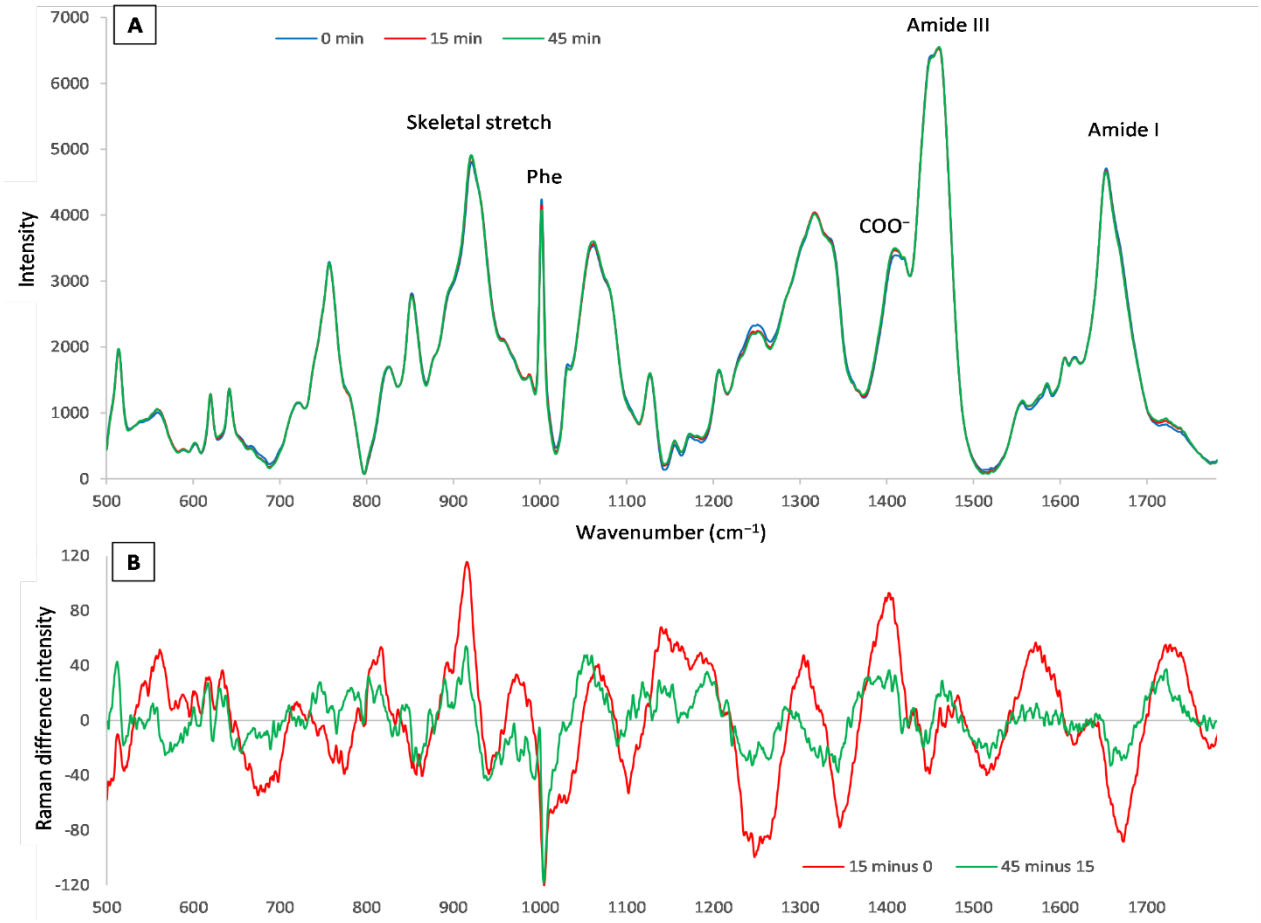

Figure 5. (A) Average Raman spectra for each incubation time from three samples in the wavenumber range from 500 to 1800 cm^{-1}. Peaks important for analyzing degree of proteolysis are noted in the figure. ***(B)*** Difference spectra for average Raman spectra for each incubation time where 15 min – 0 min and 45 min – 15 min corresponds to red and green lines, respectively.

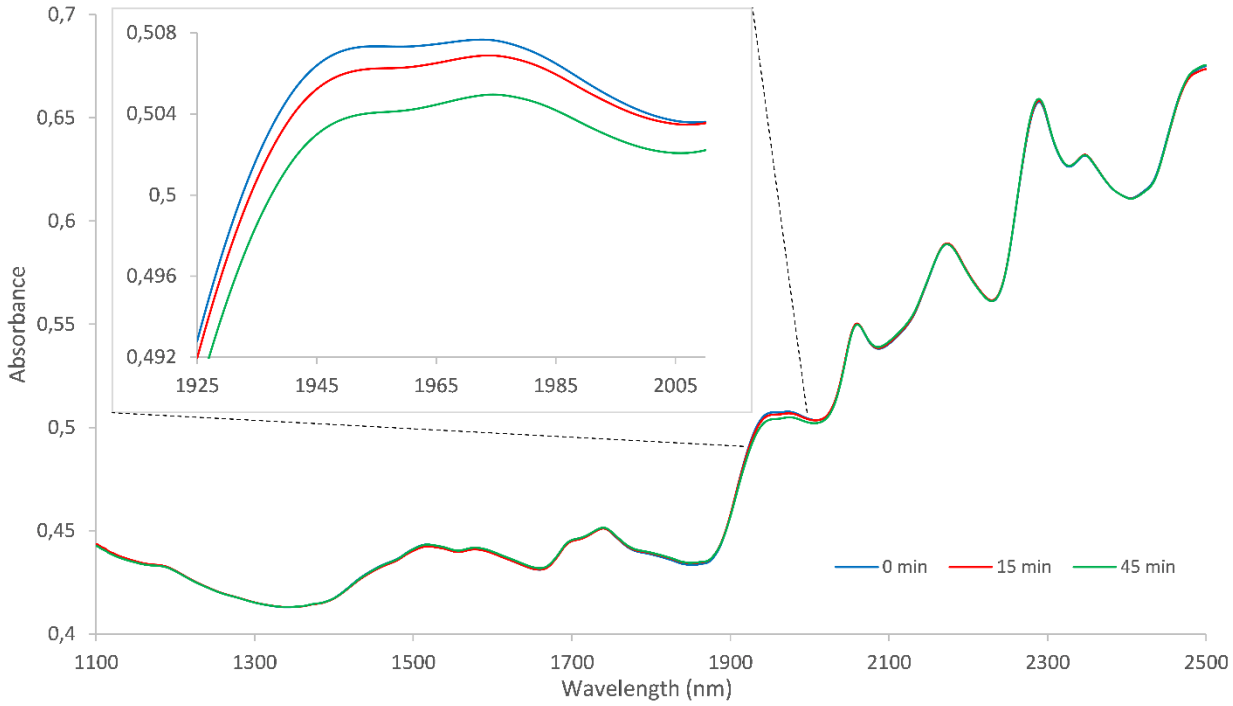

Figure 6. Average NIR spectra from dried samples after incubation for 0 min, 15 min and 45 min in the wavelength range from 1100 to 2500 nm. Inset shows the peak at approx. 1950 nm.

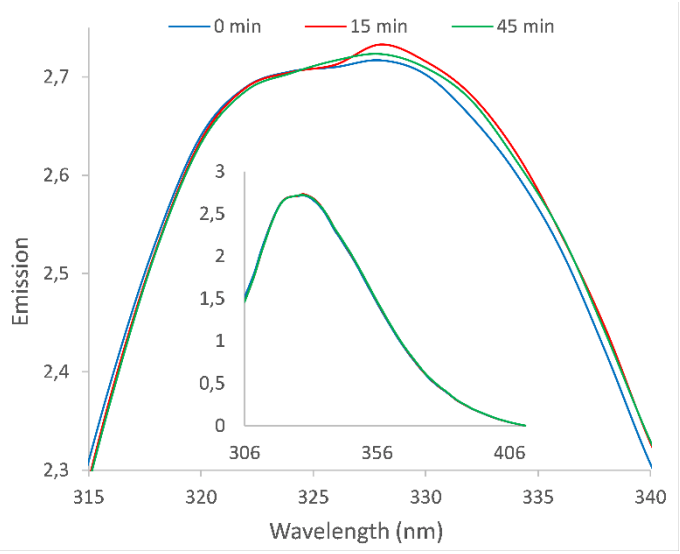

Figure 7. Average fluorescence emission spectra (excitation at 292 nm) from liquid samples for incubation at 0 min, 15 min and 45 min after SNV, shown as blue, red and green lines respectively. Inset shows entire spectra, while the main figure shows only the peak.